

Retraction

Retracted: Power Allocation Intelligent Optimization for Mobile NOMA Communication System

Journal of Advanced Transportation

Received 8 August 2023; Accepted 8 August 2023; Published 9 August 2023

Copyright © 2023 Journal of Advanced Transportation. This is an open access article distributed under the Creative Commons Attribution License, which permits unrestricted use, distribution, and reproduction in any medium, provided the original work is properly cited.

This article has been retracted by Hindawi following an investigation undertaken by the publisher [1]. This investigation has uncovered evidence of one or more of the following indicators of systematic manipulation of the publication process:

- (1) Discrepancies in scope
- (2) Discrepancies in the description of the research reported
- (3) Discrepancies between the availability of data and the research described
- (4) Inappropriate citations
- (5) Incoherent, meaningless and/or irrelevant content included in the article
- (6) Peer-review manipulation

The presence of these indicators undermines our confidence in the integrity of the article's content and we cannot, therefore, vouch for its reliability. Please note that this notice is intended solely to alert readers that the content of this article is unreliable. We have not investigated whether authors were aware of or involved in the systematic manipulation of the publication process.

Wiley and Hindawi regrets that the usual quality checks did not identify these issues before publication and have since put additional measures in place to safeguard research integrity.

We wish to credit our own Research Integrity and Research Publishing teams and anonymous and named external researchers and research integrity experts for contributing to this investigation.

The corresponding author, as the representative of all authors, has been given the opportunity to register their agreement or disagreement to this retraction. We have kept a record of any response received.

References

- [1] X. Fu, Z. Tang, and P. Xiao, "Power Allocation Intelligent Optimization for Mobile NOMA Communication System," *Journal of Advanced Transportation*, vol. 2022, Article ID 5838186, 6 pages, 2022.

Research Article

Power Allocation Intelligent Optimization for Mobile NOMA Communication System

Xiaobin Fu , Zhen Tang , and Pingping Xiao 

College of Physical Science and Engineering, Yichun University, Yichun 336000, Jiangxi, China

Correspondence should be addressed to Xiaobin Fu; fxb8508457@163.com

Received 16 March 2022; Revised 17 April 2022; Accepted 26 April 2022; Published 10 May 2022

Academic Editor: Li Feng

Copyright © 2022 Xiaobin Fu et al. This is an open access article distributed under the Creative Commons Attribution License, which permits unrestricted use, distribution, and reproduction in any medium, provided the original work is properly cited.

Non-orthogonal multiple access (NOMA) technology can greatly improve user access and spectral efficiency. This paper considers the power allocation optimization problem of a two-user mobile NOMA communication system. Firstly, a mobile NOMA communication system model is established. Then, we analyze the outage probability (OP) of mobile NOMA communication system and the relationship between OP performance and user power allocation coefficient. Finally, the optimization objective function is established, and a power allocation optimization algorithm employing monarch butterfly optimization (MBO) is proposed. Compared with firefly algorithm and artificial fish swarm algorithm, the efficiency of MBO algorithm is increased by 20.7%, which can better improve the OP performance.

1. Introduction

Recently, the number of mobile users has increased rapidly. With the rapid growth of wireless communication data, the available spectrum becomes more and more crowded, and the space in the electromagnetic spectrum will become more and more scarce [1]. To meet the high-quality communication and large-scale user access, 5G mobile communication technology has attracted extensive attention [2]. 5G mobile communication technology has been rapidly popularized with ultrahigh bandwidth, ultralarge capacity, ultralow delay, and ultraslow energy consumption, which has brought far-reaching impact and change to people's life, work, and national economic development [3, 4].

Non-orthogonal multiple access (NOMA) technology has good fairness and considerable spectral efficiency, and it is regarded as a key technology of 5G mobile communication [5–7]. A novel deep learning method was proposed to cut down the computation complexity of NOMA multiuser detection in [8]. In [9], a multiagent deep learning method was proposed to solve the complex NOMA optimization problem, which considered user fairness and decoding complexity. The authors in [10] proposed a trusted NOMA model and maximized the secure rate at the near user by

using KKT conditions. To improve the NOMA system performance, the authors in [11] proposed a joint queue-aware and channel-aware scheduling to reduce traffic delay.

Power allocation can improve the NOMA performance in [12–14]. The authors in [15] constructed a multicarrier NOMA system and proposed a power allocation algorithm to reduce computational complexity. In [16], considering an unmanned aerial vehicle (UAV)-assisted NOMA system, user grouping and power allocation were used to reduce the relative distance between users and UAV. The authors in [17] obtained the error probability to fairly allocate power to different users of the NOMA system. Considering vehicle mobility, the authors in [18] proposed a sequence-based power allocation algorithm for NOMA UAV-aided vehicular platooning. However, there are some problems in these schemes, such as large amount of calculation, poor energy efficiency performance, insufficient power utilization, and unable to balance the fairness and service quality of users.

In order to obtain the best power allocation coefficient, the swarm intelligence optimization algorithm has been widely used in [19, 20]. In [21], artificial fish swarm algorithm (AFSA) optimized a wireless sensor network coverage problem, which can reduce the energy consumption. With simplified propagation and firefly algorithm (FA), an

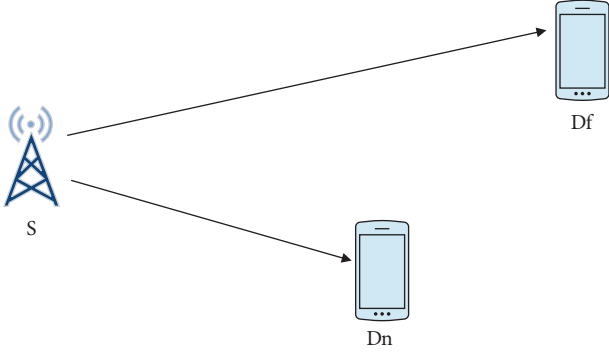


FIGURE 1: System model.

improved power point tracking algorithm was proposed in [22]. An improved cuckoo search algorithm was proposed to optimize the mobile outage probability (OP) prediction in [23]. However, these algorithms still have some shortcomings, such as low discovery rate, slow solution speed, and low solution accuracy.

Therefore, we investigate the mobile power allocation optimization. The main contributions of this paper are as follows:

- (1) A mobile NOMA communication system model is established. For ideal communication conditions, we derive the exact expressions for OP and analyze the relationship between OP and power allocation coefficient.
- (2) Considering the system efficiency and user fairness, we have established the optimization objective function. Employing monarch butterfly optimization (MBO), an intelligent optimization algorithm is proposed. MBO can reduce the computing parameters. The power allocation optimization algorithm employing MBO has good convergence performance and optimization performance.
- (3) Compared with FA and AFSA, the MBO algorithm can obtain the shortest time, which is 18.7063s, while AFSA is 48.9128s, and FA is 23.6096s. The efficiency of MBO is increased by 20.7%, which can better improve the OP performance of the mobile NOMA system.

2. System Model

Figure 1 is the mobile NOMA communication system. The system is composed of a source S, a far user Df, and a near user Dn. h_i represents the channel gains of $S \rightarrow Df$ and $S \rightarrow Dn$, $i = \{S Dn, S Df\}$. h_i is expressed as follows [24]:

$$h = \prod_{t=1}^N a_t, \quad (1)$$

where a_i is a Nakagami variable.

S transmits $\sqrt{a_1 P_s} x_1 + \sqrt{a_2 P_s} x_2$ to Df and Dn. P_s is the transmission power. a_1 and a_2 are power allocation coefficients of Df and Dn, respectively. $a_1 + a_2 = 1$, and $a_1 > a_2$.

The signals received at Df and Dn are as follows [25, 26]:

$$\begin{aligned} y_{Df} &= h_{SDf} (\sqrt{a_1 P_s} x_1 + \sqrt{a_2 P_s} x_2 + \eta_{SDf}) + v_{SDf}, \\ y_{Dn} &= h_{SDn} (\sqrt{a_1 P_s} x_1 + \sqrt{a_2 P_s} x_2 + \eta_{SDn}) + v_{SDn}, \end{aligned} \quad (2)$$

where v_{SDf} and v_{SDn} are AWGN of Df and Dn, respectively, and η_{SDf} and η_{SDn} are the distortion noise from the transmitter.

The signal-to-interference noise ratios of Df and Dn are as follows [25, 26]:

$$\begin{aligned} \gamma_{SDn} &= \frac{|h_{SDn}|^2 a_2 \gamma}{|h_{SDn}|^2 \gamma + \gamma + 1}, \\ \gamma_{SDf} &= \frac{|h_{SDf}|^2 a_1 \gamma}{|h_{SDf}|^2 a_2 \gamma + \gamma + 1}, \\ \gamma_{SDf} &= \frac{|h_{SDf}|^2 a_1 \gamma}{|h_{SDf}|^2 a_2 \gamma + \gamma + 1}, \end{aligned} \quad (3)$$

where $\gamma = P_s/N_0$ is the transmit signal-to-noise (SNR) ratio at S.

3. OP Performance Analysis

3.1. *OP of Df.* The OP of Df is expressed as

$$\begin{aligned} \text{OP}_{Df} &= \Pr(\gamma_{SDf} < \gamma_{\text{thf}}) \\ &= \Pr\left(\frac{|h_{SDf}|^2 a_1 \gamma}{|h_{SDf}|^2 a_2 \gamma + \gamma + 1} < \gamma_{\text{thf}}\right) \\ &= \Pr\left(|h_{SDf}|^2 < \frac{[\gamma + 1]\gamma_{\text{thf}}}{a_1 \gamma - a_2 \gamma \gamma_{\text{thf}}}\right) \\ &= \int_0^{[\gamma+1]\gamma_{\text{thf}}/a_1\gamma - a_2\gamma\gamma_{\text{thf}}} f_{|h_{SDf}|^2}(y) dy \\ &= F_{|h_{SDf}|^2}(y) \Big|_0^{[\gamma+1]\gamma_{\text{thf}}/a_1\gamma - a_2\gamma\gamma_{\text{thf}}} \\ &= G_{1,3}^{2,1}\left[\frac{[\gamma + 1]\gamma_{\text{thf}}}{a_1 \gamma - a_2 \gamma \gamma_{\text{thf}}} \Big|_{1, \dots, 1, 0}\right], \end{aligned} \quad (4)$$

where γ_{thf} is the interrupt threshold of Df.

3.2. *OP of Dn.* The OP of Dn is given as

$$\begin{aligned} \text{OP}_{Dn} &= \Pr(\gamma_{SDf} \rightarrow n < \gamma_{\text{thf}}, \gamma_{SDn} < \gamma_{\text{thn}}) \\ &= \Pr\left(|h_{SDn}|^2 < \frac{[\gamma + 1]\gamma_{\text{thf}}}{a_1 \gamma - a_2 \gamma \gamma_{\text{thf}}}, |h_{SDn}|^2 < \frac{[\gamma + 1]\gamma_{\text{thn}}}{a_2 \gamma - \gamma \gamma_{\text{thn}}}\right), \end{aligned} \quad (5)$$

where γ_{thn} is the interrupt threshold of Dn.

To simplify the integration process, we define the following variables:

$$\begin{aligned}\tau_1 &= \frac{[\gamma + 1]\gamma_{\text{thf}}}{a_1\gamma - a_2\gamma\gamma_{\text{thf}}}, \\ \tau_2 &= \frac{[\gamma + 1]\gamma_{\text{thn}}}{a_2\gamma - \gamma\gamma_{\text{thn}}}, \\ \tau &= \max(\tau_1, \tau_2).\end{aligned}\quad (6)$$

Bringing the above variables into (11), we obtain that

$$\begin{aligned}\text{OP}_{\text{Dn}} &= \Pr(|h_{\text{SDn}}|^2 < \tau_1, |h_{\text{SDn}}|^2 < \tau_2) \\ &= \Pr(|h_{\text{SDn}}|^2 < \max(\tau_1, \tau_2)) \\ &= \Pr(|h_{\text{SDn}}|^2 < \tau) \\ &= F_{|h_{\text{SDn}}|^2}(\tau)|_0^r \\ &= G_{1,3}^{2,1}[\tau_{1,\dots,1,0}^1].\end{aligned}\quad (7)$$

4. Intelligent Power Allocation Optimization Employing MBO Algorithm

Here, we employ the MBO algorithm to optimize the mobile power allocation.

4.1. Optimization Objective Function. To achieve high efficiency and user fairness, we should ensure $\min|\text{OP}_{\text{Df}} + \text{OP}_{\text{Dn}}|$ and $\min|\text{OP}_{\text{Df}} - \text{OP}_{\text{Dn}}|$. Therefore, the optimization objective function is

$$\min \left(\begin{array}{l} G_{1,3}^{2,1} \left[\frac{(\gamma+1)\gamma_{\text{thf}}}{a_1\gamma - a_2\gamma\gamma_{\text{thf}}} \right]_{1,\dots,1,0}^1 + G_{1,3}^{2,1}[\tau_{1,\dots,1,0}^1] \\ G_{1,3}^{2,1} \left[\frac{(\gamma+1)\gamma_{\text{thf}}}{a_1\gamma - a_2\gamma\gamma_{\text{thf}}} \right]_{1,\dots,1,0}^1 - G_{1,3}^{2,1}[\tau_{1,\dots,1,0}^1] \end{array} \right). \quad (8)$$

4.2. MBO Intelligent Optimization Algorithm. Therefore, employing the MBO algorithm, an intelligent power allocation optimization algorithm is proposed. In [27], it presents the MBO algorithm.

4.2.1. Population Initialization. The number of the monarch butterfly population is N . The number of iterations is MaxGen , and the adjustment rate is BAR .

4.2.2. Fitness Evaluation. The fitness value of each monarch butterfly individual is calculated and sorted. The sorted population is divided into two subpopulations NP_1 and NP_2 , respectively. They have N_1 and N_2 individuals, respectively.

4.2.3. New Subpopulation Generation. At the current iteration t , the NP_1 and NP_2 generate two new subpopulations, respectively. For NP_1 , it uses the migration operator to generate a new subpopulation, which is expressed as follows:

TABLE 1: Simulation parameters.

Parameter	Value
K	0
σ	0
M	1, 2, 3, 4
N	1, 2, 3, 4

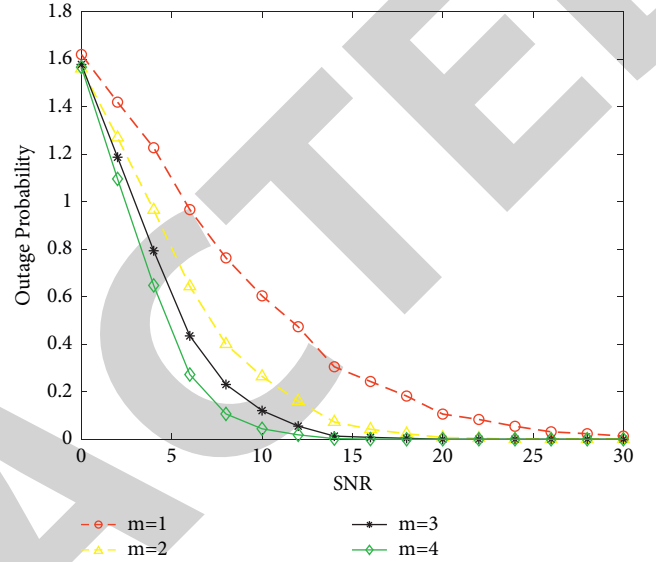


FIGURE 2: The OP performance with different (m).

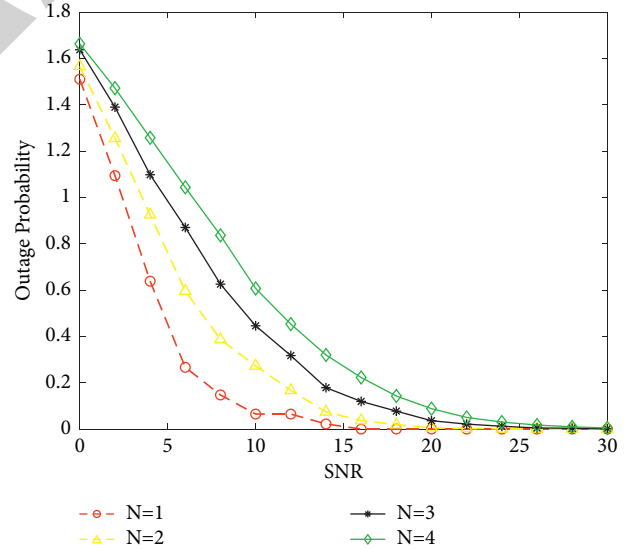


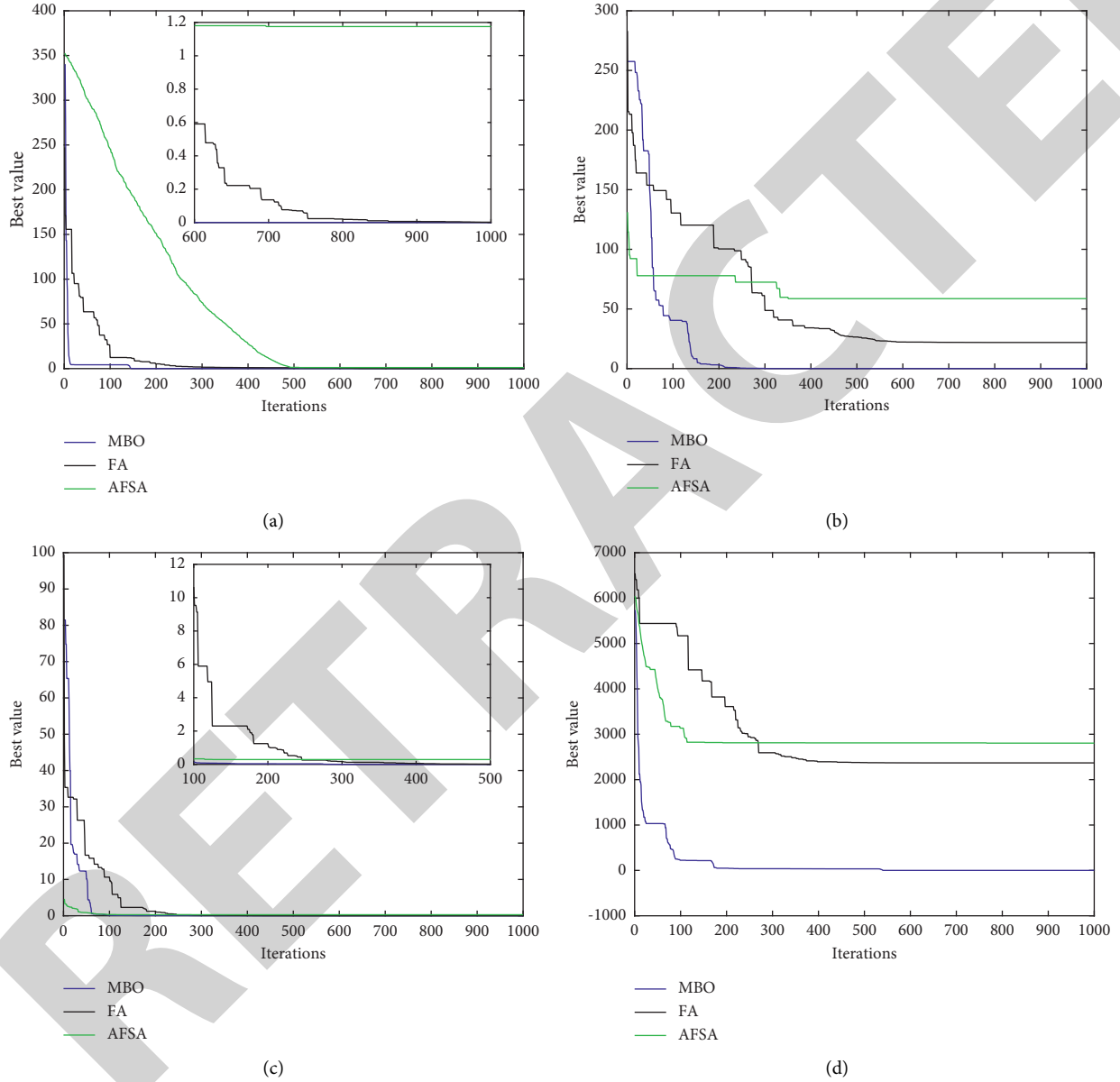
FIGURE 3: The OP performance with different (N).

$$\begin{cases} x_{i,k}^{t+1} = x_{r_1,k}^t, & r \leq p, \\ x_{i,k}^{t+1} = x_{r_2,k}^t, & \text{else,} \end{cases} \quad (9)$$

where x_{r_1} and x_{r_2} represent the k th element of r_1 and r_2 that is the newly generated position of r_1 and r_2 , respectively. r_1 and r_2 are randomly selected from NP_1 and NP_2 , respectively. r is a random number.

TABLE 2: Four test functions.

	Function	Ranges	Dimension
Griewank	$F1 = \sum_{i=1}^d x_i^2 / 4000 - \prod_{i=1}^d \cos(x_i / \sqrt{i}) + 1$	[-600, 600]	20
Rastrigin	$F2 = 10d + \sum_{i=1}^d [x_i^2 - 10 \cos(2\pi x_i)]$	[-5.12, 5.12]	20
Sphere	$F3 = \sum_{i=1}^d x_i^2$	[-500, 500]	20
Schwefel	$F4 = 418.9828d - \sum_{i=1}^d x_i \sin(\sqrt{ x_i })$	[-500, 500]	20

FIGURE 4: The convergence performance of different algorithms on F_1 - F_4 . (a) F_1 . (b) F_2 . (c) F_3 . (d) F_4 .

For NP_2 , it uses the adjustment operator to generate a new subpopulation, which is expressed as follows:

$$\begin{cases} x_{i,k}^{t+1} = x_{\text{best},k}^t, & r \leq p, \\ x_{i,k}^{t+1} = x_{r_3,k}^t, & \text{else,} \end{cases} \quad (10)$$

where x_{best} represents the position of the globally optimal individual and x_{r_3} represents the location of r_3 , which is randomly selected from NP_2 .

$rand$ is between $[0, 1]$. If $rand > BAR$, NP_2 updates $x_{i,k}^{t+1}$ again. The process is as follows:

$$\begin{cases} x_{i,k}^{t+1} = x_{i,k}^t + \beta * (dx_k - 0.5), \\ dx = \text{Levy}(x_i^{t+1}), \end{cases} \quad (11)$$

where β is the weight factor and dx represents the step size which is calculated by the Levy function.

TABLE 3: Simulation parameters for power allocation.

Parameter	Value
Iteration	1000
Population number	100
Dimension	1
Range	[0.5, 0.9]

TABLE 4: Power allocation optimization comparison.

	Optimal power allocation coefficient	Time (s)
MBO	0.56768	18.7063
FA	0.56768	23.6096
AFSA	0.56768	48.9128

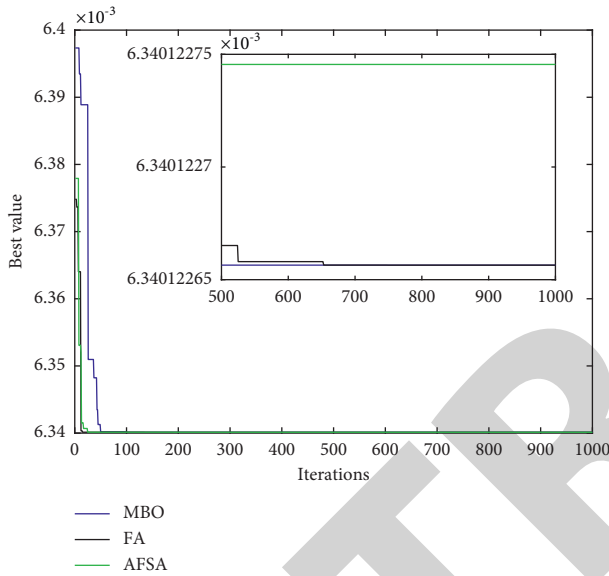


FIGURE 5: The iterative optimization process of the three algorithms.

4.2.4. New Subpopulation Merge. It merges the two newly generated subpopulations and calculates the fitness of the new population. Repeat above process, and when the number of iterations reaches $MaxGen$, the best solution is obtained.

5. Performance Analysis

This section will analyze the OP performance and optimize the power allocation using MBO, AFSA, and FA algorithms.

Table 1 gives the simulation parameters. For the ideal case, the residual hardware impairment $k=0$, and the incomplete channel state information $\sigma=0$. Figure 2 shows the OP performance with different m . From Figure 2, when the power allocation coefficient is constant, the system OP performance becomes better with the increase in SNR and m . The OP performance with different N is shown in Figure 3. As N is decreased, it can minimize the system OP.

We select four test functions, which are shown in Table 2. Figure 4 shows the convergence performance of different algorithms. For F_1 – F_4 functions, the MBO is the best.

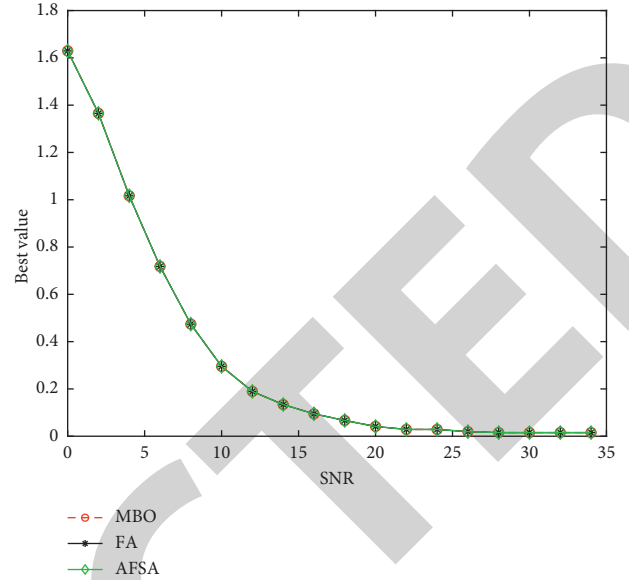


FIGURE 6: System performance comparison of the three algorithms.

Next, the power allocation will be optimized by MBO, FA, and AFSA. Table 3 shows the simulation parameters for power allocation. Table 4 shows the power allocation optimization comparison of MBO, FA, and AFSA algorithms. Compared with FA, MBO has a 20.7% decrease. The iterative optimization process of the MBO, FA, and AFSA algorithms is shown in Figure 5.

The system performance comparison of the MBO, FA, and AFSA algorithms is shown in Figure 6. From Figure 6, the performance of the MBO algorithm is good, which is the same as FA and AFSA algorithms. However, the MBO algorithm has a low complexity.

6. Conclusion

This paper studies the power allocation optimization for the mobile NOMA communication system. Firstly, the mobile NOMA model is built, and the OP expressions for D_f and D_n are derived. Then, the optimization objective function is established, and a power allocation optimization algorithm is proposed. Finally, it can obtain the best power allocation coefficient. The efficiency of the MBO algorithm is improved by 20.7%.

Data Availability

The data used to support the findings of this study are available from the corresponding author upon reasonable request and with permission of funders.

Conflicts of Interest

The authors declare that they have no conflicts of interest.

Acknowledgments

This project was supported by the National Natural Science Foundation of China (No. 11664043).

References

- [1] P. K. Hota, S. Thapar, and D. Mishra, R. Saini and A. Dubey, Ergodic performance of downlink untrusted NOMA system with imperfect SIC," *IEEE Communications Letters*, vol. 26, no. 1, pp. 23–26, 2022.
- [2] J. Nightingale, P. Salva-Garcia, J. M. A. Calero, and Q. Wang, "5G-QoE: QoE modelling for ultra-HD video streaming in 5G networks," *IEEE Transactions on Broadcasting*, vol. 64, no. 2, pp. 621–634, 2018.
- [3] E. Garro, M. Fuentes, J. L. Carcel et al., "5G mixed mode: NR multicast-broadcast services," *IEEE Transactions on Broadcasting*, vol. 66, no. 2, pp. 390–403, 2020.
- [4] L. Chettri and R. Bera, "A comprehensive survey on internet of things (IoT) toward 5G wireless systems," *IEEE Internet of Things Journal*, vol. 7, no. 1, pp. 16–32, 2020.
- [5] X. W. Li, Z. Xie, Z. Chu, V. G. Menon, S. Mumtaz, and J. H. Zhang, "Exploiting benefits of IRS in wireless powered NOMA networks," *IEEE Transactions on Green Communications and Networking*, vol. 6, no. 1, 2022.
- [6] Z. Hong, G. Li, Y. Xu, and X. Zhou, "User grouping and power allocation for downlink NOMA-based quadrature spatial modulation," *IEEE Access*, vol. 8, no. 2020, pp. 38136–38145, 2020.
- [7] Y. Sun, D. W. K. Ng, Z. Ding, and R. Schober, "Optimal joint power and subcarrier allocation for full-duplex multicarrier non-orthogonal multiple access systems," *IEEE Transactions on Communications*, vol. 65, no. 3, pp. 1077–1091, 2017.
- [8] Y. Bai, W. Chen, B. Ai, Z. Zhong, and I. J. Wassell, "Prior information aided deep learning method for grant-free NOMA in mMTC," *IEEE Journal on Selected Areas in Communications*, vol. 40, no. 1, pp. 112–126, 2022.
- [9] X. Xu, Q. Chen, X. Mu, Y. Liu, and H. Jiang, "Graph-embedded multi-agent learning for smart reconfigurable THz MIMO-NOMA networks," *IEEE Journal on Selected Areas in Communications*, vol. 40, no. 1, pp. 259–275, 2022.
- [10] I. Amin, D. Mishra, R. Saini, and S. Aissa, "QoS-aware secrecy rate maximization in untrusted NOMA with trusted relay," *IEEE Communications Letters*, vol. 26, no. 1, pp. 31–34, 2022.
- [11] Y. Liu, W. Chen, and J. Lee, "Joint queue-aware and channel-aware scheduling for non-orthogonal multiple access," *IEEE Transactions on Wireless Communications*, vol. 21, no. 1, pp. 264–279, 2022.
- [12] M. Alibeigi, A. Taherpour, and S. Gazor, "Improving secrecy rate and social welfare by NOMA technique in D2D communications network," *IEEE Transactions on Green Communications and Networking*, 2021, <https://ieeexplore.ieee.org/document/9638994>.
- [13] L. W. Xu, X. P. Zhou, Y. Li, F. Cai, X. Yu, and N. Kumar, "Intelligent power allocation algorithm for energy-efficient mobile internet of things (IoT) networks," *IEEE Transactions on Green Communications and Networking*, 2022.
- [14] H. Wang, P. Xiao, and X. Li, "Channel parameter estimation of mmWave mimo system in urban traffic scene: a training channel-based method," *IEEE Transactions on Intelligent Transportation Systems*, pp. 1–9, 2022.
- [15] E. C. Cejudo, H. Zhu, and J. Wang, "Resource allocation in multicarrier NOMA systems based on optimal channel gain ratios," *IEEE Transactions on Wireless Communications*, vol. 21, no. 1, pp. 635–650, 2022.
- [16] G. Q. Li, J. Z. Lin, Y. J. Xu, Z. W. Huang, and T. Liu, "User grouping and power allocation algorithm for UAV-aided NOMA network," *Journal on Communications*, vol. 41, no. 9, pp. 21–28, 2020.
- [17] T. Analooei, S. M. Saberali, and M. Majidi, "Multi-threshold detector with fair power allocation coefficients for NOMA signals with statistical CSI," *IEEE Communications Letters*, vol. 25, no. 12, pp. 3970–3974, 2021.
- [18] Y. Sun, K. Zheng, and Y. Tang, "Control efficient power allocation of uplink NOMA in UAV-aided vehicular platooning," *IEEE Access*, vol. 9, no. 10, pp. 139473–139488, 2021.
- [19] M. Y. Arafat and S. Moh, "Localization and clustering based on swarm intelligence in UAV networks for emergency communications," *IEEE Internet of Things Journal*, vol. 6, no. 5, pp. 8958–8976, 2019.
- [20] L. Xu, X. Yu, and T. A. Gulliver, "Intelligent outage probability prediction for mobile IoT networks based on an IGWO-elman neural network," *IEEE Transactions on Vehicular Technology*, vol. 70, no. 2, pp. 1365–1375, 2021.
- [21] Y. Feng, S. Zhao, and H. Liu, "Analysis of network coverage optimization based on feedback K-means clustering and artificial fish swarm algorithm," *IEEE Access*, vol. 8, no. 1, pp. 42864–42876, 2020.
- [22] Y.-P. Huang, M.-Y. Huang, and C.-E. Ye, "A fusion firefly algorithm with simplified propagation for photovoltaic MPPT under partial shading conditions," *IEEE Transactions on Sustainable Energy*, vol. 11, no. 4, pp. 2641–2652, 2020.
- [23] L. Xu, H. Wang, and T. A. Gulliver, "Outage probability performance analysis and prediction for mobile IoV networks based on ICS-BP neural network," *IEEE Internet of Things Journal*, vol. 8, no. 5, pp. 3524–3533, 2021.
- [24] G. K. Karagiannidis, N. C. Sagias, and P. T. Mathiopoulos, "\$N_{\text{last}}\$Nakagami: a novel stochastic model for cascaded fading channels," *IEEE Transactions on Communications*, vol. 55, no. 8, pp. 1453–1458, 2007.
- [25] X. Li, M. Liu, D. Deng, J. Li, C. Deng, and Q. Yu, "Power beacon assisted wireless power cooperative relaying using NOMA with hardware impairments and imperfect CSI," *AEU - International Journal of Electronics and Communications*, vol. 108, no. 8, pp. 275–286, 2019.
- [26] J. Men, J. Ge, and C. Zhang, "Performance analysis for downlink relaying aided non-orthogonal multiple access networks with imperfect CSI over Nakagami- m fading," *IEEE Access*, vol. 5, no. 5, pp. 998–1004, 2017.
- [27] G.-G. Wang, S. Deb, and Z. Cui, "Monarch butterfly optimization," *Neural Computing & Applications*, vol. 31, no. 7, pp. 1995–2014, 2019.